

# Thermoelastic Stress: How Important As a Cause of Earthquakes in Young Oceanic Lithosphere?

STEVEN R. BRATT,<sup>1</sup> ERIC A. BERGMAN, AND SEAN C. SOLOMON

*Department of Earth, Atmospheric and Planetary Sciences, Massachusetts Institute of Technology, Cambridge*

We present a series of exploratory models which test the hypothesis that thermoelastic stress is a significant contributor to the state of stress in young oceanic lithosphere (less than 35 m.y. in age). In support of this hypothesis is the concentration of seismicity in lithosphere younger than 15 m.y. where cooling rates are relatively high. Most near-ridge earthquakes have focal depths between the Moho and the depth of the 800°C isotherm. Thrust and strike-slip events dominate the shallowest seismicity, while the focal mechanisms of the deeper events are generally characterized by normal faulting. To assess the importance of thermal stress in the generation of near-ridge earthquakes, we model the lithosphere as an elastic half-space in which the response to cooling is computed using the method of thermoelastic displacement potentials. A key assumption in the models is that stress is relieved on time scales generally short compared with the age of the lithosphere. A further assumption in some models is that material will not contribute thermal stress until it has cooled below an elastic blocking temperature. Normal faulting is predicted throughout the lithosphere in thermal stress models based on simple half-space cooling. Models in which a cooled surface layer is incorporated to simulate the effect of hydrothermal circulation on shallow thermal structure predict stresses that can match the locations of both thrust- and normal-faulting earthquakes near mid-ocean ridges. The addition of a "ridge push" stress to the computed thermal stress enhances the likelihood of thrust faulting in the uppermost lithosphere at ages greater than about 15 m.y. but probably contributes little to the stress field at younger ages. Though these simple models are limited by several simplifying assumptions, particularly in the immediate vicinity of the ridge axis, they support the hypothesis that thermoelastic stress can play a major role in the tectonics of young oceanic lithosphere.

## INTRODUCTION

A potentially important contributor to the state of stress in oceanic lithosphere is thermoelastic or thermal stress. Thermal stress can develop in the elastic portion of young oceanic lithosphere because of differential cooling and contraction. It has been proposed as a major contributor to the formation of transform faults [Turcotte, 1974; Collette, 1974], the propagation of mid-plate island and seamount chains [Turcotte and Oxburgh, 1973], and the generation of earthquakes in older oceanic lithosphere [Sykes and Sbar, 1974]. Thermal stress generated during plate cooling has not been explicitly included in most global stress models [e.g., Richardson *et al.*, 1979; Fleitout and Froidevaux, 1983], in large part because of the expectation that thermal stress would tend to be relieved at young lithosphere ages and, once relieved, would not be renewed [e.g., Solomon *et al.*, 1975].

Recent determinations of the mechanisms and focal depths of earthquakes in young oceanic lithosphere [Bergman *et al.*, 1984; Wiens and Stein, 1984; Bergman and Solomon, 1984] have led us to reexamine the role of thermal stress. Specifically, the distribution of source mechanisms with depth and with distance from the ridge axis in oceanic lithosphere 2–35 m.y. old appears to be generally consistent with the hypothesis that many of these earthquakes represent the response of the brittle portion of the lithosphere to accumulated thermal stress [Bergman and Solomon, 1984]. In this paper, we present several simple models for the state of thermoelastic stress in young oceanic lithosphere, and we compare the predictions of

these models with the characteristics of near-ridge earthquakes.

## CHARACTERISTICS OF NEAR-RIDGE EARTHQUAKES

The principal source of data on the state of stress in young oceanic lithosphere consists of the source mechanisms and focal depths of near-ridge earthquakes. Detailed and comprehensive studies of the source mechanisms of such earthquakes have recently been completed by Bergman and Solomon [1984] and by Wiens and Stein [1984]. The data of Bergman and Solomon [1984], obtained from an inversion of long-period *P* and *SH* wave forms for 32 events from 1962–1981 in oceanic lithosphere 2.5–35 m.y. old, are summarized in Figure 1. Individual data points are accurate to about  $\pm 2$  km in centroid depth and generally  $\pm 2$  m.y. in age; for a few events located near fracture zones or in poorly surveyed regions the uncertainty in lithosphere age is greater [Bergman and Solomon, 1984].

On the basis of the results shown in Figure 1, several generalizations may be made. Most near-ridge earthquakes, and nearly all of those with seismic moments greater than  $10^{25}$  dyn cm, occur in lithosphere less than 15 m.y. old. The majority of near-ridge events are located at mantle depths (greater than 6–7 km below the seafloor). While all styles of faulting are observed, there appears to be an approximate stratification of fault types. Thrust faulting is confined to the uppermost 10 km; compressional axes both nearly parallel to and oblique to the local spreading direction are seen. Most of the strike-slip mechanisms occur at intermediate depths within the seismically active portion of young oceanic lithosphere. The deepest earthquakes at any age display predominantly normal faulting mechanisms; tensional axes are either oblique or perpendicular to the direction of spreading. The centroid depths of the normal faulting events appear to be bounded by the depth to an isotherm of about 800°C as calculated from standard half-space or plate cooling models [e.g., Turcotte and

<sup>1</sup> Now at Science Applications International Corporation, San Diego, California.

Copyright 1985 by the American Geophysical Union.

Paper number 4B5329.  
0148-0227/85/004B-5329\$05.00

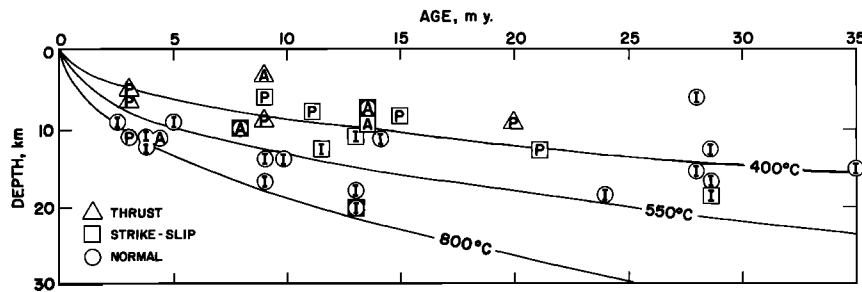


Fig. 1. Centroid depth and focal mechanism type versus lithosphere age for 32 near-ridge earthquakes [Bergman and Solomon, 1984]. Depths are relative to the seafloor. Earthquakes are further distinguished on the basis of the ocean in which they occur (A, Atlantic, I, Indian, P, Pacific). Mechanism symbols are superposed for earthquakes showing a mixture of faulting types. Also shown are selected isotherms from the half-space cooling model of (1).

Oxburgh, 1967; Parsons and Sclater, 1977]. A large fraction of near-ridge earthquakes during the last 20 years, particularly of events with normal faulting mechanisms, has occurred in the central Indian Ocean. A high level of intraplate seismicity in the Indian Ocean in both old and young lithosphere may be attributable in part to enhanced levels of lithospheric stress associated with the ongoing collision between India and Asia [Stein and Okal, 1978; Weissel et al., 1980; Bergman et al., 1984]. Generally similar distributions of mechanism type and centroid depth with age in the smaller data sets from the Atlantic and Pacific oceans, however, suggest that an explanation should be sought for the patterns displayed in Figure 1 that is not peculiar to any particular oceanic region.

#### SOURCES OF STRESS IN OCEANIC LITHOSPHERE

The tectonics of oceanic lithosphere are not the product of any single source of stress. Contributions to the total state of stress arise from such sources as shear tractions at the base of the lithosphere [e.g., Richter and Parsons, 1975; Hager and O'Connell, 1979], latitudinal components of plate motions [Turcotte and Oxburgh, 1973], crustal thickness and lithospheric density variations [Artyushkov, 1973], lithospheric loading and unloading [Walcott, 1970; Watts and Cochran, 1974], and some combination of pull [McKenzie, 1969; Turcotte and Schubert, 1971] and resistance [Smith and Toksoz, 1972; Forsyth and Uyeda, 1975] at subduction zones and transform faults. Many of these processes are local in their effects and thus would not be expected to contribute to a globally consistent pattern of faulting in young oceanic lithosphere.

Perhaps the most pervasive sources of stress in young oceanic lithosphere are those related to plate cooling. These include both thermal stress [Turcotte and Oxburgh, 1973; Turcotte, 1974] and the compression, or "ridge push," that results from the elevation of mid-ocean ridges and the lateral heterogeneity of lithospheric density [e.g., Hales, 1969; McKenzie, 1972; Dahlen, 1981]. Because the effects of these processes depend predominantly on the thermal structure and material properties of the plate, ridge push and thermoelastic stress should depend primarily on age and on depth and should be more or less consistent from ocean to ocean.

The stress field resulting from the elevation of a mid-ocean ridge relative to adjacent cooler and denser lithosphere has been evaluated by Dahlen [1981] under the assumption that deviatoric stress in the lithosphere is the minimum necessary to support the lateral variations in density and bathymetry produced by cooling. For a two-dimensional model of cooling lithosphere the principal deviatoric stresses are compressional in the direction of spreading, extensional and equal in mag-

nitude in the vertical direction, and zero parallel to the ridge. At any given age the deviatoric stresses are maximum at the seafloor and decrease with depth. The surface deviatoric stress reaches about 200 bars at an age of 30 m.y. In contrast to thermal stress the stress associated with ridge push is "renewable" [Bott and Kusznir, 1984]; i.e., it is not significantly relieved by brittle failure. We consider below the relative importance of thermal stress and ridge push in the near-ridge environment.

#### PREVIOUS MODELS OF THERMAL STRESS

As young oceanic lithosphere spreads from the ridge, it cools nonuniformly and, as a result, is subjected to thermal stress. Previously published models of thermal stress either have been qualitative in nature [Sykes and Sbar, 1974; Collette, 1974; Epp and Suyenaga, 1978] or have been taken from simple analytic solutions based on restrictive assumptions [Turcotte and Oxburgh, 1973; Turcotte, 1974]. The most developed such model is that of Turcotte [1974], according to which the ridge is assumed to be two-dimensional and to have a prescribed zero-age temperature profile. The normal component of stress in the direction parallel to the ridge ( $\sigma_{yy}$ ) is taken to be the only nonzero principal stress. Thermal stress at each point is assumed to be the result only of local thermal contraction due to cooling below an elastic "blocking temperature" [see also Turcotte, 1983]. The local stress in this model thus does not depend on the state of stress in surrounding material.

Turcotte [1974] considered the possibility that the product of Young's modulus  $E$  and thermal expansion coefficient  $\alpha$  differs between crust and mantle, in particular, that  $\alpha E$  in the mantle is larger than  $\alpha E$  in the crust. If so, a discontinuity in  $\sigma_{yy}$  is developed, with the highest extensional stresses occurring immediately beneath the Moho. As a result, the lithosphere acts as a bimetallic strip. In the absence of bending, the accumulated thermal stress  $\sigma_{yy}$  is everywhere extensional and can exceed 1 kbar at 2 m.y. age and 3 kbar at 20 m.y. As the largest extensional thermal stresses are relieved by fracture, the net force on the lithosphere (the integral of  $\sigma_{yy}$  over depth) must be zero, driving the upper part of the elastic plate into horizontal compression in the  $y$  direction. The age and depth of the transition from compression to extension depend on the assumed temperature profile at the ridge, the physical constants assumed for crust and mantle material, and the detailed history of stress relief.

The simple thermal stress model of Turcotte [1974] is in reasonable qualitative agreement with the earthquake data of Figure 1, including the depth dependence of thrust and normal faulting mechanisms and the tendency of the  $P$  and  $T$

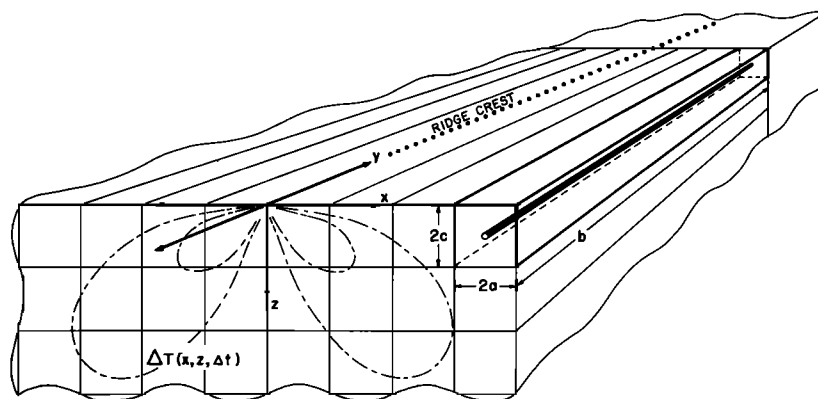


Fig. 2. Geometry of the thermoelastic stress problem for cooling oceanic lithosphere; see text.

axes, respectively, for these earthquakes to be oblique or perpendicular to the spreading direction. Several of the assumptions made by *Turcotte* [1974], however, are not likely to be valid. The component of thermal stress in the direction of spreading cannot be neglected, except perhaps very near the ridge axis. To the extent that the upper lithosphere behaves elastically, the stress at each point must also depend on the deformation and state of stress in surrounding material. Further, the relatively high level of seismicity in young oceanic lithosphere suggests that thermal stresses are not accumulated indefinitely but may rather be at least partly relieved by recurring earthquake activity. For these reasons, a more complete treatment of thermal stress in young oceanic lithosphere is desirable.

#### CALCULATION OF THERMAL STRESS

In this section we describe a new approach to the estimation of thermal stress in oceanic lithosphere. The stress models are based on the elastic response to heterogeneous cooling of oceanic lithosphere. The basic model is that of a cooling elastic half-space, though we also consider a simple modification to the assumed temperature field to account approximately for the effects of hydrothermal circulation. Various assumptions are made regarding an effective elastic blocking temperature [*Turcotte*, 1974, 1983] and the time scale for relief of thermal stress by fracture. A number of different thermal stress models resulting from these parameter variations are considered. For each model we compare the predicted state of stress with that indicated by the mechanisms and locations of earthquakes depicted in Figure 1. On the basis of these comparisons we assess the contribution of thermoelastic stress to the tectonics in young oceanic lithosphere.

#### Temperature Structure

For most of the thermal stress models the adopted temperature structure is that of a simple cooling half-space [e.g., *Turcotte and Oxburgh*, 1967]:

$$T(x, z) = T_L \operatorname{erf} \left[ \frac{z}{2} \left( \frac{v}{k|x|} \right)^{1/2} \right] \quad (1)$$

where erf is the error function,  $T_L$  is the temperature at the ridge axis and at large depth  $z$ , and  $k$  is the thermal diffusivity. The coordinate system is illustrated in Figure 2. The lithosphere is taken to spread in the  $\pm x$  direction outward from the ridge at  $x = 0$  at the half rate  $v$ . Depth is relative to the

seafloor, at which the temperature is a constant  $0^\circ\text{C}$ . The  $y$  direction is parallel to the ridge crest. Values for all adopted physical parameters are given in Table 1. Selected isotherms given by (1) are shown in Figure 1; this simple thermal structure has been shown to be consistent with seafloor depth versus age for lithosphere younger than 80 m.y. [*Davis and Lister*, 1974; *Parsons and Sclater*, 1977].

A complication of the simple cooling model represented by (1) which may significantly affect the resulting thermal stress field arises from hydrothermal circulation in the uppermost lithosphere. Hydrothermal circulation acts to cool a substantial fraction of the crust at or near the ridge axis [*Lister*, 1972, 1977], so that the zero-age temperature appropriate to the calculation of thermal stress is significantly cooler than (1) to some uncertain (and perhaps variable) depth. Limited data from the depths of ridge crest microearthquakes [*Lilwall et al.*, 1978; *Toomey et al.*, 1985] and from oxygen isotope measurements in ophiolite samples [*Gregory and Taylor*, 1981] suggest that hydrothermal circulation extends at least to the Moho for some ridge systems. Heat flow data indicate that hydrothermal circulation continues to maintain a low conductive gradient at the top of the lithosphere to ages as great as 80 m.y. [*Anderson et al.*, 1977]. To approximate the effects of ridge axis cooling by hydrothermal circulation, we consider as a simple alternative to the thermal structure given by equation (1) the following model:  $T = 0^\circ\text{C}$  for  $z < h$ , and  $T$  is given by (1) with  $z - h$  substituted for  $z$  in the argument of the error function for  $z > h$ . We have examined models in which  $h = 5$  and  $h = 10$  km. A similar thermal model has been employed by *Lewis* [1983] in his calculation of gravity anomalies over ridge structures. While the model of a uniform  $0^\circ\text{C}$  temperature in the hydrothermally cooled layer is surely incorrect in

TABLE 1. Adopted Values of Parameters Used in Thermal Stress Models [*Parsons and Sclater*, 1977]

Variable	Description	Value
$k$	Thermal diffusivity	$8 \times 10^{-3} \text{ cm}^2/\text{s}$
$T_L$	Temperature at ridge crest and beneath the lithosphere	$1350^\circ\text{C}$
$v$	Spreading half rate	1 cm/yr
$\alpha$	Volumetric coefficient of thermal expansion	$3.2 \times 10^{-5}/^\circ\text{C}$
$E$	Young's modulus	$1.7 \times 10^{12} \text{ dyn/cm}^2$
$\nu$	Poisson's ratio	0.25
$g$	Gravitational acceleration	$980 \text{ cm/s}^2$
$\rho_m$	Density of uncooled lithosphere	$3.33 \text{ g/cm}^3$

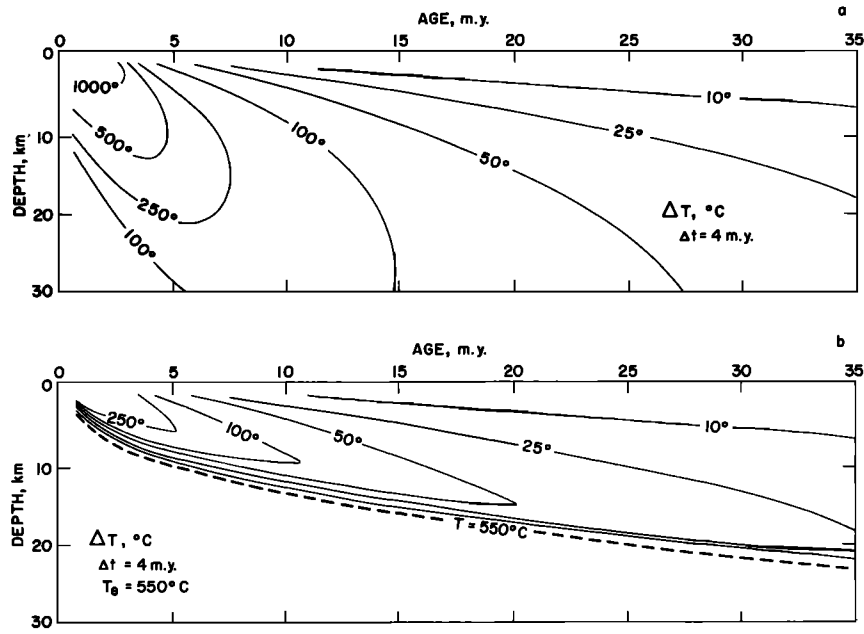


Fig. 3. (a) Temperature change  $\Delta T$  in a cooling half-space over a time increment  $\Delta t$  of 4 m.y., from (9). (b) Same as Figure 3a except that temperatures above an elastic "blocking temperature" of 550°C do not contribute to  $\Delta T$  (see text).

detail, the critical element of this model for the thermal stress calculation is that the temperature field from the surface to the depth  $h$  does not vary significantly with lithosphere age.

#### Thermoelastic Displacement Potentials

To estimate thermal stress, we employ the method of thermoelastic displacement potentials developed originally by Goodier [1937]. The response of an infinite, elastic solid to a nonuniform temperature change  $\Delta T(x, y, z)$  can be represented by a distribution of centers of contraction (or dilatation) of magnitude

$$\theta = \frac{\alpha \Delta T (1 + \nu)}{12\pi (1 - \nu)} \quad (2)$$

where  $\alpha$  is the volumetric coefficient of thermal expansion and  $\nu$  is Poisson's ratio (Table 1). The solution to the thermal stress problem in a semi-infinite solid requires that the surface be free of tractions. To satisfy these boundary conditions, a center of contraction, a double force, and a doublet, each appropriately weighted, are applied at the image point  $(x, y, -z)$  corresponding to every center of contraction  $(x, y, z)$  within the half-space [Mindlin and Cheng, 1950]. The displacement field  $\mathbf{u}$  is given by

$$\mathbf{u} = -\nabla\phi_1 - \nabla_2\phi_2 \quad (3)$$

where the thermoelastic displacement potentials

$$\phi_1 = \iiint_{V'} \frac{\theta}{R_1'} dx' dy' dz' \quad (4)$$

$$\phi_2 = \iiint_{V'} \frac{\theta}{R_2'} dx' dy' dz'$$

are integrals of  $\theta$  over volume  $V$  in the half-space, weighted by the inverse of the distance scalars

$$R_1' = [(x - x')^2 + (y - y')^2 + (z - z')^2]^{1/2}$$

$$R_2' = [(x - x')^2 + (y - y')^2 + (z + z')^2]^{1/2}$$

The vector operator applied to  $\phi_2$  is

$$\nabla_2\phi_2 = (3 - 4\nu)\nabla\phi_2 + 2\nabla\left(z\frac{\partial\phi_2}{\partial z}\right) - 4(1 - \nu)\nabla^2(z\phi_2)\mathbf{e}_k$$

where  $\nabla^2$  is the scalar Laplacian and  $\mathbf{e}_k$  is the unit vector in the  $z$  direction.

It may be seen from (3) that given a temperature distribution for which the potential is known, the displacement field can be readily calculated by differentiation. To model the elastic response of cooling lithosphere, we divide the half-space into rectangular boxes (Figure 2) within which the temperature change  $\Delta T$  is assumed to be constant and for which the potential may be determined. The total displacement field can then be computed by summing the displacements due to the temperature changes in individual boxes. While the thermoelastic displacement potential for a uniformly cooled box is known [MacMillan, 1930], the solution involves 36 terms containing various trigonometric and logarithmic functions. To reduce computation time, we approximate the potential of a uniformly cooled box by that of a line source [MacMillan, 1930]. The potential at  $(x, y, z)$  due to a line source of strength  $4ac\theta$  located at  $(x', y' = 0, z')$  and oriented parallel to the  $y$  axis is given by

$$\phi_1 = 4ac\theta \ln \left[ \frac{S_1 - (y - b)}{S_2 - (y + b)} \right] \quad (5)$$

where

$$S_1 = [(x - x')^2 + (y - b)^2 + (z - z')^2]^{1/2}$$

$$S_2 = [(x - x')^2 + (y + b)^2 + (z - z')^2]^{1/2} \quad (6)$$

and where  $a$ ,  $b$ , and  $c$  are the half widths of the box represented by the line source in the  $x$ ,  $y$ , and  $z$  directions, respectively (Figure 2). The corresponding expression for  $\phi_2$  differs only by the substitution of  $(z + z')$  for  $(z - z')$  in (6).

We have tested the accuracy of this approximation by comparing the displacement field produced by a cooling sphere embedded in a half-space [Mindlin and Cheng, 1950] with that predicted by the cooling of an embedded cube of equal

volume assembled by the superposition of line sources given by (5) and representing boxes of various cross-sectional shapes. This procedure was repeated using different volumes and burial depths. The line source approximation to the potential of a box was found to be best when the represented box has a nearly square cross section with sides that are small in relation to the distance ( $R_1$ ) between the observation point and the box. Following these criteria, the calculated displacements (radial and vertical) induced by the cooling of an embedded cube of half length  $L$  differ from those due to the cooling of an embedded sphere of volume  $8L^3$  by about 1% at a distance of  $0.1L$  from the center of either figure, 5% at a distance of  $0.6L$ , 5% at a distance of  $2L$ , and less than 1% at a distance of  $2.5L$ . On the basis of this test we believe that the approximation to (4) is generally accurate to within a few percent for arbitrary two-dimensional temperature fields.

### Thermal Stress

The thermal stress resulting from differential cooling is calculated from the displacement field given by (3) using standard formulae [e.g., *Timoshenko and Goodier*, 1970, p. 456]. The normal strains and stresses are of the form

$$\epsilon_{xx} = \partial u / \partial x$$

etc.

$$\sigma_{xx} = -\frac{E}{(1+\nu)(1-2\nu)} \left[ (1-\nu)\epsilon_{xx} + \nu(\epsilon_{yy} + \epsilon_{zz}) - \frac{\alpha}{3}(1+\nu)\Delta T(x, y, z) \right] \quad (7)$$

etc., where  $\mathbf{u} = (u, v, w)$ ,  $E$  is Young's modulus (Table 1), and compressional stresses are positive. By restricting our consideration to the plane of symmetry  $y = 0$  (Figure 2),  $\sigma_{xy}$  and  $\sigma_{yz}$  vanish and  $\sigma_{yy}$  is a principal stress. The shear strain and stress in the  $x-z$  plane are given by

$$\begin{aligned} \epsilon_{xz} &= \frac{1}{2} \left( \frac{\partial u}{\partial z} + \frac{\partial w}{\partial x} \right) \\ \sigma_{xz} &= -\frac{E}{1+\nu} \epsilon_{xz} \end{aligned} \quad (8)$$

From (7) and (8) the magnitudes and directions of principal stresses may be calculated [e.g., *Fung*, 1977, pp. 91–108] and the principal deviatoric stresses  $\sigma_1$  (greatest compressive stress),  $\sigma_2$ , and  $\sigma_3$  (greatest extensional stress) derived. The style of faulting expected at any location follows from the stress deviators [*Anderson*, 1951]. Throughout the discussion below, all principal stresses are deviatoric stresses unless otherwise stated.

In order to compare the predicted thermal stress field with the near-ridge earthquake data of Figure 1 we make the assumption that thermal stress is generally relieved on time scales short compared to the age of the lithosphere. This relief of stress presumably occurs by brittle failure in the upper part of the lithosphere and by ductile flow in the lower part; the earthquakes depicted in Figure 1 are a primary manifestation of the brittle component of this stress relief process. In the terminology of *Bott and Kusznir* [1984], thermal stress is non-renewable: Once such stress is relieved, only the subsequently accumulated stress contributes to the future stress state. Relief of stress in the oceanic lithosphere undoubtedly occurs by several processes that operate on a variety of time scales. For simplicity, however, we parameterize this process by a single

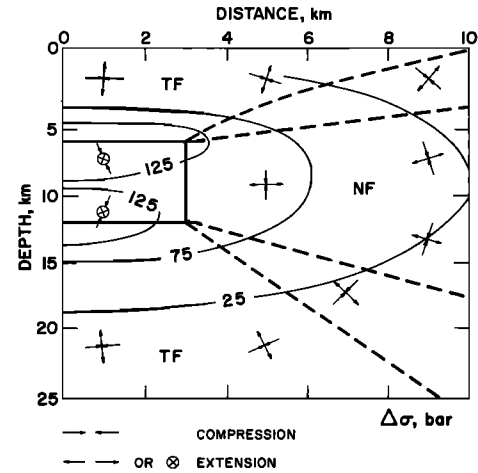


Fig. 4. Thermal stress in an elastic half-space due to the cooling of an elongated box 6 km by 6 km in cross section. The box is centered at  $x = 0$ ,  $y = 0$ , and  $z = 9$  km and has  $x$ ,  $y$ , and  $z$  half dimensions  $a = 3$ ,  $b = 10.000$ , and  $c = 3$  km, respectively. The initial temperature within the box is  $10^\circ\text{C}$ , while that of the rest of the half-space and of the surface is  $0^\circ\text{C}$ ; the thermal stress shown is at large  $t$  after all cooling is complete. The orientations of the greatest ( $\sigma_1$ ) and least ( $\sigma_3$ ) compressive deviatoric stresses are indicated by arrows. Also shown are contours in bars of the differential stress  $\Delta\sigma = \sigma_1 - \sigma_3$ . Zones of predicted thrust (TF) and normal faulting (NF) are outlined by dashed lines.

characteristic time  $\Delta t$ , independent of depth or lithosphere age, for relief of thermal stress. In this time interval, the temperature of a parcel of lithosphere (i.e., in a Lagrangian frame) changes by the amount

$$\Delta T(x, z, \Delta t) = T(x, z) - T(x - v \Delta t, z) \quad (9)$$

where  $T(x, z)$  is taken from one of the thermal models described earlier. The quantity  $\Delta T$  is independent of  $y$ , is symmetric about  $x$ , and tends to zero with increasing  $x$  and  $z$ . The magnitude of  $\Delta T$  is approximately linear with  $\Delta t$  for locations distant from the ridge axis. Values of  $\Delta T$  for the half-space cooling model are given in Figure 3a for  $\Delta t = 4$  m.y.

We calculate the thermal stress accumulated during the time interval  $\Delta t$  by substituting relation (9) into (2)–(3) and (5)–(8). With this approach,  $\Delta t$  may be regarded as a parameterized recurrence time for total relief of stress. In lithosphere younger than  $\Delta t$ , (9) is modified so that stress accumulation occurs over a time equal to the lithosphere age.

The thermal stress field computed from equations (2)–(3) and (5)–(9) will be valid only if the rocks subjected to the temperature change  $\Delta T$  behave elastically over the entire temperature range. It is more likely, however, that at high temperatures, stress will be relieved by ductile flow and thus will not be transmitted to surrounding regions. While we cannot account for this flow explicitly in the elastic model employed in this paper, we can simulate its effect by postulating that a parcel of lithosphere does not contribute to the stress field until it cools below an elastic blocking temperature  $T_e$  [*Turcotte*, 1974, 1983]. By this postulate the magnitudes of  $T(x, z)$  and  $T(x - v \Delta t, z)$  in (9) are restricted not to exceed  $T_e$ , and the deepest nonzero contour of  $\Delta T$  will follow closely the  $T = T_e$  isotherm. We take  $T_e$  to be the isotherm approximately marking the base of the mechanically strong lithosphere. For an assumed stress difference of 500 bars, *McNutt and Menard* [1982] concluded that  $T_e \approx 550^\circ\text{C}$  if laboratory deformation measurements can be extrapolated to geological strain rates.

TABLE 2. Models of Thermal Stress in Young Oceanic Lithosphere

Model	Hydrothermal Circulation?	$\Delta t$ , m.y.	$T_e$ , °C	Ridge Push?	Figure
A	no	4	$T_L$	no	5
B	yes	4	$T_L$	no	6
C	no	4	550	no	7
D	yes	4	550	no	8
E	yes	10	550	no	9
F	yes	4	550	yes	11

Contours of  $\Delta T$  (that portion of the temperature change that contributes to thermal stress) for  $\Delta t = 4$  m.y. and  $T_e = 550^\circ\text{C}$  are shown in Figure 3b. The limitations of including a blocking temperature as a means of accounting for high-temperature anelastic behavior are discussed further below.

#### Assessment of Procedure

The procedures described above for the estimation of thermal stress involve several oversimplifications to the actual behavior of cooling oceanic lithosphere. A significant limitation of the model is the assumption that the oceanic lithosphere can be represented as a uniform elastic half-space. Because of the consequent continuity of displacements and stresses across the ridge axis, strains produced on one side of the ridge axis affect the stress field in the adjacent plate. The effect of the assumed elasticity of the ridge axis region, however, will primarily be confined to the vicinity of the ridge; as demonstrated by equations (3)–(8), the strain produced by a contracting element falls off with distance as  $1/R^2$ . A stress-free boundary or wedge along the ridge axis would be preferable to a uniform elastic half-space, but such a modification cannot be readily accommodated within the scheme adopted here.

Two potentially important contributors to the lithospheric stress field which we have not included are variations in physical properties (e.g., between crust and mantle) and plate bending. As shown by *Turcotte* [1974], these effects can modify the thermal stress field in oceanic plates. Similarly, temperature- and depth-dependent rheology cannot be represented in a simple model such as that presented here, but the use of an elastic blocking temperature provides a rough approximation to the effects of stress relaxation by ductile flow. The time interval over which stress accumulates before failure is not likely to be uniform throughout the oceanic lithosphere, as is assumed in our model. Rather, the characteristic time for relief of stress must be a function of depth and age because of the dependence of mechanism and rate of deformation on temperature, effective pressure, strain rate, and state of stress [*Brace and Kohlstedt*, 1980]. Stress may accumulate over relatively long time intervals without failure in lithospheric regions where rates of cooling and strain are small and temperatures are low. The characteristic time for stress release may be considerably less near the ridge crest, where both temperatures and strain rates are relatively high and where at least the upper crust is likely to be cracked and porous and therefore weak [e.g., *Lister*, 1977; *Goetze and Evans*, 1979]. We return to this point below in the discussion of individual models.

The thermal stress models in this paper do not include the effects of offsets or of modifications to the thermal structure at transform faults or fracture zones. Although such effects might be incorporated into the procedures used here by superposing cooling blocks in three dimensions to approximate actual distributions of seafloor ages, we do not consider such compli-

cations in this paper. The models below are therefore appropriate only to regions far from fracture zones and transforms where temperature gradients in the  $y$  direction are negligible. A further concern is the possibility that transform faults and fracture zones are regions where the mechanical strength is low and the assumption of elasticity is invalid. While this possibility is open for transforms, profiles of bathymetry and gravity across inactive fracture zones indicate that the elastic lithosphere is essentially continuous across such features [*Sandwell and Schubert*, 1982].

The procedure for calculation of thermal stress adopted in this paper has several advantages over earlier, simpler models. Whereas the models of *Turcotte and Oxburgh* [1973] and *Turcotte* [1974] consider the thermal stress due only to contraction at each point in isolation, the stress field determined here includes the contributions to stress from deformation in the surrounding medium. Furthermore, the method of thermoelastic displacement potentials enables us to consider the complete stress tensor without the need to make a priori assumptions about the magnitude of any particular stress component. Finally, it is straightforward to include a characteristic time for release of thermal stress. Through this characteristic time parameter we can also scale the predicted magnitude of thermal stress to time-independent stress fields such as that arising from ridge push.

#### THERMAL STRESS MODELS

We now consider a suite of models for thermal stress that incorporate the various assumptions and parameterizations discussed above. As an instructive precursor to full stress models of oceanic lithosphere we first briefly consider the thermoelastic stress resulting from the cooling of a simple elongated box within an otherwise uniform half-space (Figure 4). The stress field can be regarded as an approximate Green's function, which when convolved with a distribution of temperature changes such as those given by (9) will yield the full thermal stress field in the oceanic lithosphere problem. The magnitude of the thermal stress field scales with the initial temperature of the box ( $10^\circ\text{C}$ ). The box, 6 by 6 km in the  $x$  and  $z$  directions, is approximated by nine line sources of half length  $b = 10,000$  km spaced 2 km apart in  $x$  and  $z$ . Within the cooling box all principal values of the full stress tensor are extensional. Strain in the  $y$  direction is negligible within the box because the problem is nearly two-dimensional; as a result,  $\sigma_3$  is in the  $y$  direction. Above and below the box are regions of horizontal compression; zones of horizontal extension are present on either side. In general, the  $\sigma_3$  directions outside the cooling box tend to be oriented toward the box center.

Models for the thermal stress field in oceanic lithosphere can be thought of as a superposition of stress fields of the sort depicted in Figure 4, each weighted by the appropriate change in temperature. We consider a suite of models that variously incorporate the assumptions and parameters discussed earlier (Table 2), including half-space cooling, a cold layer over a cooling half-space to simulate the effects of hydrothermal circulation, an elastic blocking temperature, different characteristic times for release of stress, and the superposition of ridge push. In all of the models below, the temperature and stress models are essentially two dimensional ( $b = 10,000$  km). Thus  $\epsilon_{yy}$  is small, and the models should be regarded as most applicable to regions of oceanic lithosphere at some distance from transform faults and fracture zones.

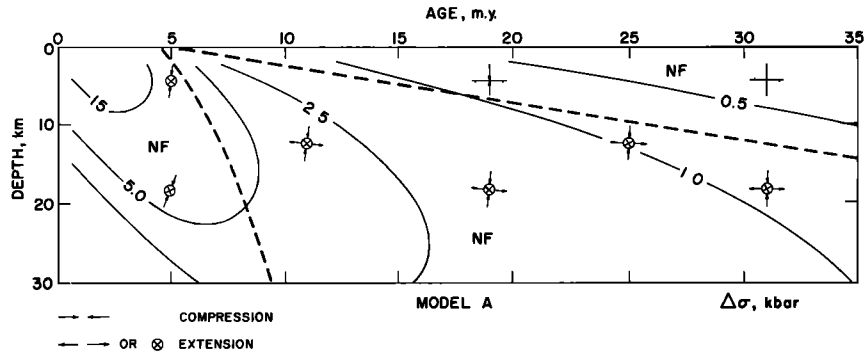


Fig. 5. Predicted thermal stress for model A, including only simple half-space cooling. The model is symmetric about  $x = 0$ . The orientations of greatest ( $\sigma_1$ ) and least ( $\sigma_3$ ) compressive stress are indicated; three directions are shown when two of the principal stresses are comparable in magnitude. Also shown are contours of the differential stress  $\Delta\sigma$  in kilobars; a characteristic time scale  $\Delta t$  of 4 m.y. for release of accumulated thermal stress has been assumed. Zones of predicted thrust (TF), strike-slip (SS), and normal (NF) faulting are outlined by dashed lines.

### Half-Space Cooling

We first explore the thermal stress resulting from simple half-space cooling (model A). No elastic blocking temperature (i.e.,  $T_e = T_L$ ) and no hydrothermally cooled layer (i.e.,  $h = 0$ ) are included. The deviatoric stress field for  $\Delta t = 4$  m.y. is shown in Figure 5. The principal values of the full stress tensor are everywhere extensional, and the two nearly horizontal principal stresses are similar in magnitude and larger by 1–2 orders of magnitude than the nearly vertical principal stress. This stress state can be understood by considering a distribution of simple cooling boxes of the type depicted in Figure 4, weighted according to the distribution of incremental temperature given in Figure 3a. The state of generally horizontal deviatoric extension (Figure 5) is partly a consequence of the large temperature changes occurring near the ridge, which in the elastic solution act to pull material at greater ages toward the axis. This effect is magnified in the half-space model because the continuity of normal stress across the ridge axis allows contraction on one side of the ridge to produce strains, the largest of which is  $\epsilon_{xx}$ , in material on the opposite side. The extension induced by near-ridge cooling is larger than the horizontal deviatoric compression contributed above any single cooling element (see Figure 4).

In Figure 5, normal faulting is predicted for all regions shown. Of course, ductile flow rather than brittle failure is likely to be the dominant mechanism of strain release in those portions of the lithosphere at temperatures greater than 600°–800°C, i.e., the lower left corner of the figure (see Figure 1). Because  $\sigma_2$  and  $\sigma_3$  are both extensional and are similar in magnitude (within 50%) throughout much of the lithosphere

in model A, the predicted  $T$  axes of normal faulting earthquakes produced by this stress field could vary in orientation from directions parallel to directions perpendicular to the spreading direction, with the result probably dependent on contributions from local sources of stress. The maximum differential stress  $\Delta\sigma$  at each lithospheric age occurs at the depth where the temperature change  $\Delta T$  is greatest. The magnitude of differential stress depends on the assumed characteristic time for release of stress. For  $\Delta t = 4$  m.y. (Figure 5),  $\Delta\sigma$  exceeds 5 kbar in 8-m.y.-old lithosphere and exceeds 1 kbar at 30 m.y. age. Very near the ridge axis, the rapidly changing temperature field predicts differential stresses in excess of 10 kbar for this model. It is likely, however, that accumulated stress will be released on a time scale much shorter than 4 m.y. in this part of the lithosphere, so such large stresses need never be sustained.

Model A thus matches the observed normal faulting mechanisms and the variable orientation of the  $T$  axes relative to the spreading direction for the deeper near-ridge earthquakes depicted in Figure 1. Any model with a constant  $\Delta t$  will account approximately for the decrease in the release of seismic moment with increasing lithosphere age because the time rate of change of temperature and therefore the thermal stress also decrease rapidly with age. A more physically reasonable model would incorporate failure criteria that depend on depth and age. In such a model the increasing strength of the lithosphere and the approach to thermal equilibrium would lead to a corresponding increase in  $\Delta t$  with age, or a decline in the predicted rate of thermally-driven seismicity.

While model A is broadly consistent with the pattern of

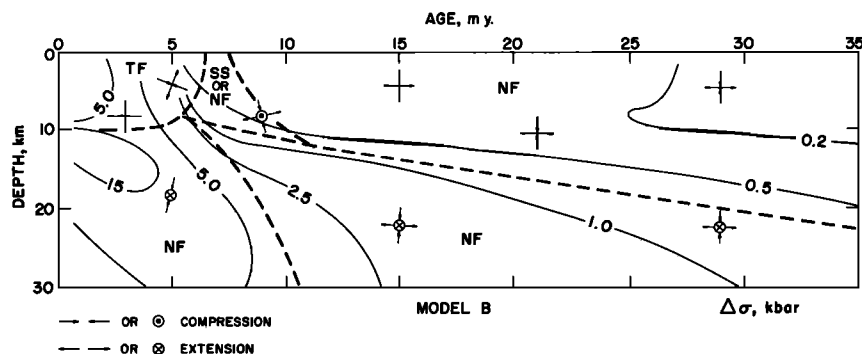


Fig. 6. Predicted thermal stress for model B. The model includes a 10-km-thick cooled layer ( $\Delta T = 0$ ) to simulate hydrothermal circulation. See Figure 5 for further explanation.

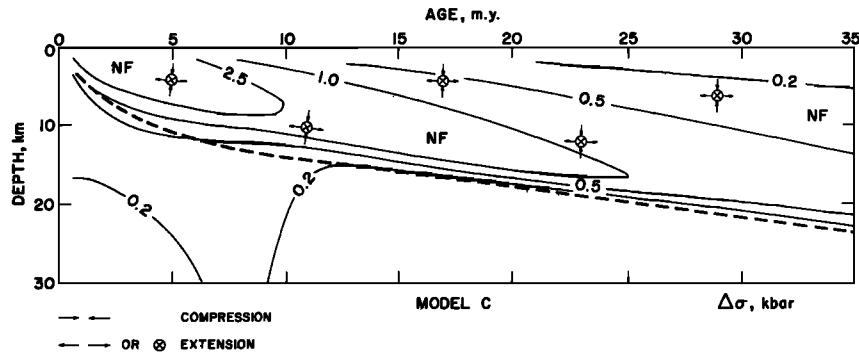


Fig. 7. Predicted thermal stress for model C. An elastic blocking temperature  $T_e = 550^\circ\text{C}$  has been assumed (see text). No hydrothermally cooled layer is present. See Figure 5 for further explanation.

normal faulting earthquakes it fails to predict horizontal deviatoric compression. The model is thus not consistent with the observation of thrust and strike-slip earthquakes within the uppermost 12 km of young oceanic lithosphere (Figure 1).

#### Effect of a Hydrothermally Cooled Layer

We next consider a thermal stress model (B) that differs from model A by its incorporation of the approximate effect of cooling of a surficial layer by hydrothermal circulation at the ridge axis. The direction of principal stresses and magnitude of deviatoric stress for model B are shown in Figure 6. The model incorporates a cold layer ( $\Delta T = 0$ ) 10 km thick and a characteristic time  $\Delta t$  for stress release of 4 m.y. Because the isotherms are depressed in relation to simple halfspace cooling, model B predicts a near-ridge region where  $\sigma_1$  is nearly horizontal. The effect is similar to that illustrated by the simple box model of Figure 4 in which contraction within the box leads to horizontal compression in the region above. A zone of predicted thrust faulting in young shallow lithosphere extends to ages just greater than  $\Delta t$ , or about 6 m.y., for model B. With increasing lithosphere age, the direction of maximum extension rotates increasingly toward the horizontal, a consequence of the large temperature changes and associated thermal strains near the ridge axis. For  $\Delta t = 4$  m.y.,  $\Delta\sigma$  exceeds 5 kbar in 5-m.y.-old lithosphere and is greater than 1 kbar at depth in lithosphere 25 m.y. in age. The pattern of stresses below 10 km depth is similar to that in model A shifted deeper by about 10 km.

Many of the characteristics of the stress field inferred from earthquake focal mechanisms (Figure 1) are reasonably well matched by model B. Within the region dominated by normal faulting, the horizontal deviatoric stresses  $\sigma_2$  and  $\sigma_3$  are similar in magnitude (to within 50%), in agreement with the vari-

able orientation of  $T$  axes observed for normal faulting earthquakes. Thrust and strike-slip failure is predicted out to 10 m.y. in age and to depths where these earthquake styles are observed in young lithosphere. Because the depth to which hydrothermal circulation cools the lithosphere determines the depth extent of horizontal deviatoric compression, a thinner hydrothermally cooled layer would not fit the earthquake observations as well as model B. In the real earth, hydrothermal cooling probably does not penetrate to a constant depth in all oceanic lithosphere; the regions of thrust and strike-slip faulting may be areas where the effects of hydrothermal cooling have penetrated to the greatest depths. The simplicity of the cooling and stress models, however, should discourage drawing significant conclusions on the depth extent of hydrothermal circulation solely from these results.

Within the region of thrust faulting, model B predicts that the  $P$  axes should be in the direction of spreading, in agreement with the mechanisms of about half of the thrust-faulting earthquakes observed to date in young oceanic lithosphere and all such events well removed from major transform faults [Bergman and Solomon, 1984; Wiens and Stein, 1984]. A problem with model B is that the magnitude of  $\Delta\sigma$  is small and that only normal faulting is predicted in the upper 10–20 km of lithosphere at ages substantially greater than  $\Delta t$ . In particular, the thrust and strike-slip earthquakes observed between 8 and 20 m.y. in age (Figure 1) are not predicted by model B.

#### Effect of an Elastic Blocking Temperature

As discussed earlier, lithospheric material at temperatures above some "blocking" temperature  $T_e$  may not contribute significantly to the thermal stress field [Turcotte, 1974, 1983]. We therefore consider next a model (C) for thermal stress in oceanic lithosphere that is similar to model A except that an

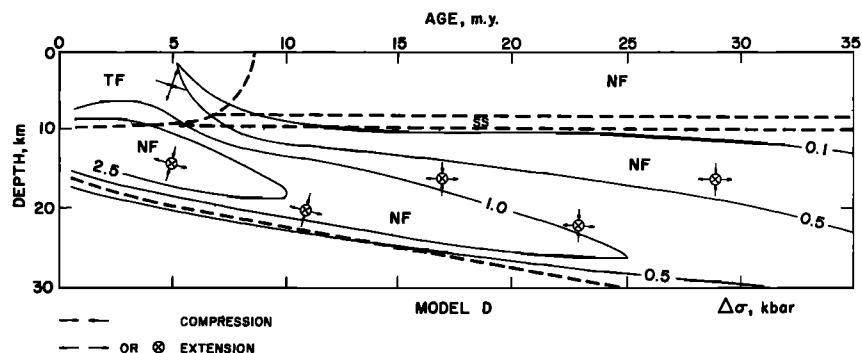


Fig. 8. Predicted thermal stress for model D. The model includes an elastic blocking temperature  $T_e = 550^\circ\text{C}$  and a hydrothermally cooled layer 10 km in thickness. See Figure 5 for further explanation.

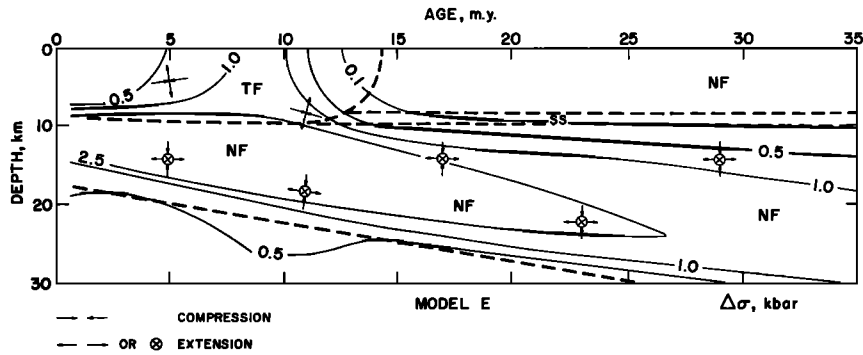


Fig. 9. Predicted thermal stress for model *E*. The model is similar to *D* except that  $\Delta t = 10$  m.y. See Figure 5 for further explanation.

elastic blocking temperature  $T_e$  of  $550^\circ\text{C}$  is assumed. The directions of principal stresses and magnitude of differential stress for model *C* are shown in Figure 7.

Differences between models *A* and *C* can be attributed entirely to differences in  $\Delta T$  (compare Figures 3a and 3b). In general, the differential stress in model *C* is small in magnitude at depths greater than that of the  $550^\circ\text{C}$  isotherm. (That the thermal stress is nonzero below this depth is a result of the elastic half-space solution.) This pattern is in qualitative agreement with the distribution with depth and age of near-ridge earthquakes (Figure 1), though the precise isotherm corresponding to the greatest depth of earthquake activity depends strongly on the cooling model. For simple half-space cooling this isotherm is between  $700^\circ$  and  $800^\circ\text{C}$  [Chen and Molnar, 1983; Wiens and Stein, 1983, 1984; Bergman and Solomon, 1984]. In contrast to model *C*, model *A* predicts differential stresses in excess of several kilobars in deep regions of young lithosphere where earthquakes are not observed.

In model *C* the magnitudes of  $\sigma_2$  and  $\sigma_3$  are more nearly equal (within 20%) than in models *A* and *B*. The predicted  $T$  axis of a normal faulting earthquake (at a depth above the  $550^\circ\text{C}$  isotherm) could lie at any azimuth between the  $x$  and  $y$  axes, in agreement with observations. As with model *A*, however, no thrust or strike-slip failure is predicted in the upper part of the lithosphere.

We consider simultaneously the effects of a hydrothermally cooled layer and an elastic blocking temperature in model *D* (Figure 8). Model *D* predicts a stress field not unlike that of model *B* (Figure 6), except that the magnitude of  $\Delta\sigma$  is everywhere less and stresses decrease rapidly at depths corresponding to temperatures greater than  $T_e$ . Because of the approach used here to simulate the effect of hydrothermal circulation, isotherms are deeper by  $h$  at all ages in relation to those

shown in Figures 1 and 3b. It is interesting to note that the resulting location of the  $T_e = 550^\circ\text{C}$  isotherm follows closely the locus of the deepest observed near-ridge earthquakes (Figure 1) when  $h = 5$  to 10 km, so that the seismic and laboratory measures of the base of the elastic lithosphere are in near agreement.

Within the normal faulting regime of model *D*, the magnitudes of  $\sigma_2$  and  $\sigma_3$  differ by less than 20%, consistent with the observed pattern of normal faulting. The region of predicted thrust failure extends to almost 9 m.y. in age, though the magnitude of  $\Delta\sigma$  drops rapidly at ages greater than  $\Delta t$  (4 m.y.). Again, the predicted direction of thrusting in the model is the  $x$  direction. A region of strike-slip failure is predicted at the base of the hydrothermal region. This may be compared with a concentration of strike-slip earthquakes observed in lithosphere 8 to 21 m.y. old between 5 and 12 km depth (Figure 1). The value of  $\Delta\sigma$ , however, is less than 100 bars over much of the strike-slip region in model *D*.

#### Increasing the Characteristic Time for Stress Release

Model *E* is identical to model *D* except that the characteristic time  $\Delta t$  for stress release is 10 m.y. rather than 4 m.y. The stress field and predicted faulting patterns for model *E* are shown in Figure 9. The predicted stress magnitudes increase with increasing  $\Delta t$ , while the sense of faulting is generally independent of  $\Delta t$  at ages greater than this quantity. The greater period of stress accumulation before release, however, leads to a field of thrust and strike-slip faulting that extends to greater age than in model *D*. Thrust faulting is predicted to about 14 m.y. in age, and  $\Delta\sigma$  remains greater than 500 bars until about 12 m.y. Most of the zone of strike-slip failure is, as in model *D*, characterized by small differential stress. Normal faulting with a variable  $T$  axis direction is predicted below 10

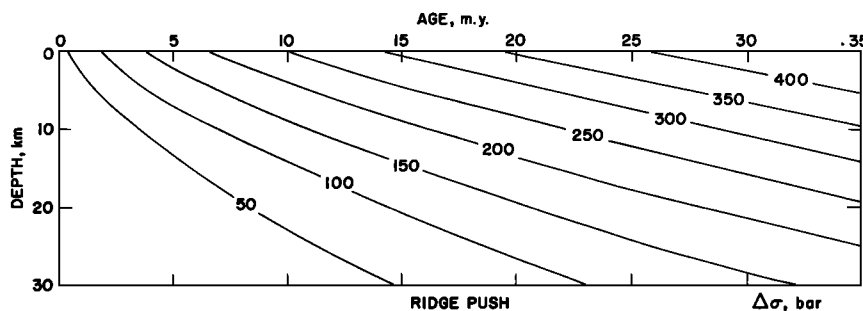


Fig. 10. Stress field predicted from the ridge push model of Dahlen [1981]. Contours represent lines of constant stress difference  $\Delta\sigma = \sigma_{xx} - \sigma_{zz}$ . The principal deviatoric stresses  $\sigma_{xx}$  and  $\sigma_{zz}$  in this model have magnitudes equal to  $\Delta\sigma/2$  and are opposite in sign.

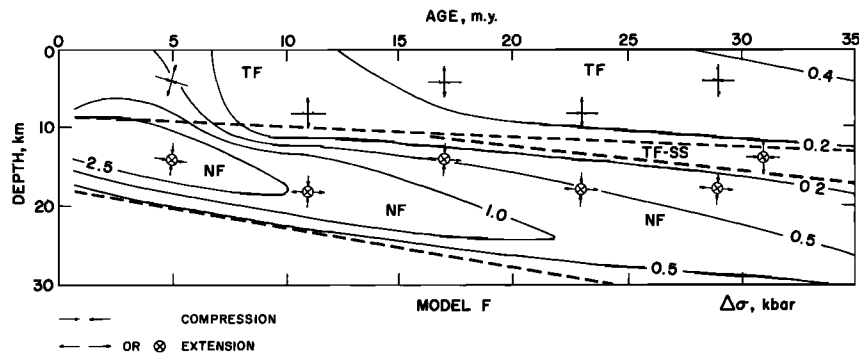


Fig. 11. Predicted stress field for model *F*. The model is a superposition of the thermal stress from model *D* and the ridge push stress field from Figure 10. See Figures 5 and 10 for further explanation.

km depth. With  $\Delta t = 10$  m.y., in excess of 2.5 kbar of differential stress is permitted to accumulate within the normal faulting field in lithosphere 25 m.y. old. The orientations of principal stresses in model *E* are in approximate agreement with those inferred from the mechanisms of near-ridge earthquakes (Figure 1). Because of the large and uniform value of  $\Delta t$ , however, the observed age dependence of moment release for young oceanic lithosphere is not as well matched by this model as by earlier ones.

#### Contribution of Ridge Push

As discussed above, thermoelastic stress is not the sole contributor to the state of stress in young oceanic lithosphere. In particular, ridge push forces resulting from the elevation of ridge crests and the associated horizontal density variations in oceanic lithosphere represent a persistent source of stress that may play an important contributing role in the distribution of seismicity and earthquake focal mechanisms. The horizontal deviatoric compression and vertical deviatoric extension generated by ridge push should enhance, to some degree, the likelihood of thrust failure in the upper 10–15 km of oceanic lithosphere.

*Dahlen* [1981] derived an expression for the state of stress resulting from ridge push forces under the assumptions that  $\sigma_{xx}$  and  $\sigma_{zz}$  are the only nonzero terms in the deviatoric stress tensor, that the lithosphere is in a state of isostatic equilibrium, and that deviatoric stresses within the lithosphere have relaxed to the minimum necessary to support the lateral variations in bathymetry and density. The stress field contributed by ridge push is then

$$\sigma_{xx} = -\sigma_{zz} = g\alpha T_L \rho_m \left( \frac{k|x|}{v} \right)^{1/2} \text{ierfc} \left[ \frac{z}{2} \left( \frac{v}{k|x|} \right)^{1/2} \right] \quad (10)$$

where  $g$  is gravitational acceleration,  $\rho_m$  is the density of uncooled lithosphere (i.e., at  $T = T_L$ ), and the function  $\text{ierfc}$  is the first integral of the complementary error function [Gautschi, 1964].

Contours of equal  $\Delta\sigma = \sigma_{xx} - \sigma_{zz}$  predicted from (10) are plotted in Figure 10. Adopted values of the necessary physical parameters are given in Table 1. Compression in the direction of spreading increases with age and decreases with depth. The magnitude of differential stress in the crust is in excess of 200 bars by 10 m.y. in age and 400 bars by 30 m.y. In the regions of young lithosphere where thrust and strike-slip events dominate failure (5–12 km depth, 3–20 m.y. in age),  $\Delta\sigma$  ranges from about 50 to 250 bars.

If ridge push forces strongly influenced seismic failure in young oceanic lithosphere, one would expect an increase in thrust faulting with increasing plate age. Because the mechanisms of near-ridge earthquakes display no such pattern, *Bergman and Solomon* [1984] concluded that the stress differences typical of oceanic lithosphere less than 35 m.y. in age probably exceed the stress differences produced by ridge push alone. By this reasoning, in stress models that combine thermal stress and ridge push we should seek thermal stress contributions having  $\Delta\sigma$  in excess of 200–400 bars for lithosphere ages between 15 and 35 m.y. In the context of the models of this paper the scaling of thermal stress to any renewable source of stress is through the characteristic time  $\Delta t$  for stress release. This condition on  $\Delta\sigma$  is satisfied by values for  $\Delta t$  in the vicinity of several million years.

A stress model *F* consisting of the superposition of the ridge push stress field of Figure 10 with the thermal stress field of model *D* (Figure 8) is depicted in Figure 11. The most significant changes in this model compared to model *D* are the expansion of the shallow thrust faulting field to encompass all lithosphere ages and an increase in the magnitude of  $\Delta\sigma$  in the uppermost lithosphere. Within the region of predicted thrust faulting,  $\Delta\sigma$  decreases with increasing age for ages less than about 10 m.y. and increases (more slowly) with age for ages greater than 10 m.y. as ridge push begins to dominate thermal stress in the uppermost lithosphere. The *P* axes of thrust faulting earthquakes predicted by the model are in the direction of spreading, a result consistent with the focal mechanisms of thrust events far from transform faults. The thin zone of predicted strike-slip faulting is somewhat deeper in model *F* than in model *D*; the zone of predicted normal faulting is quite similar in the two models.

#### DISCUSSION

##### Comparison of Predicted and Observed Strain Rates

While the above models for thermal stress are capable of explaining many of the characteristics of the distribution and mechanisms of near-ridge earthquakes, an important independent question is whether the release of thermal stress can account quantitatively for the rate of release of seismic moment in young oceanic lithosphere. The rate of moment release may be related approximately to the average rate of shear strain within a volume undergoing a homogeneous style of faulting. *Molnar* [1983] and *Kostrov* [1974] have shown that if a region of volume  $V$  is transected by faults on which the sense of slip during earthquakes is uniform, the maximum rate of shear strain experienced by the region during a time interval  $t$

is given by

$$\dot{\epsilon}_{\max} = \frac{\Sigma M_0}{\mu V t} \quad (11)$$

where  $\mu$  is the shear modulus and  $\Sigma M_0$  is the sum of the seismic moments of earthquakes within the volume during that time interval.

We have evaluated (11) separately for lithosphere less than 15 m.y. in age and 15–35 m.y. in age and for the depth intervals characterized predominantly by thrust faulting and predominantly by normal faulting. We have included seismic moments from the compilation of *Bergman and Solomon* [1984], appropriate to  $t = 20$  years. For consistency with Table 2, we take  $\mu = 6.8 \times 10^{11}$  dyn/cm<sup>2</sup>. To estimate  $V$ , we take the areas of seafloor in each age range from *Sclater et al.* [1980], and we assume that the thickness of the volume in question is 5 km for the thrust faulting regime and 10 km for the normal faulting regime. With these assumptions,  $\dot{\epsilon}_{\max}$  is  $1 \times 10^{-18}$  s<sup>-1</sup> and  $2 \times 10^{-19}$  s<sup>-1</sup> for the portion of oceanic lithosphere experiencing normal faulting in the age ranges 0–15 and 15–35 m.y., respectively; the corresponding figure for the portion experiencing thrust faulting in the age range 0–15 m.y. is  $2 \times 10^{-18}$  s<sup>-1</sup>. (Only one thrust faulting event is shown in Figure 1 for the 15- to 35-m.y. age interval.)

These figures may be compared with the corresponding rates of thermal strains predicted by the thermal stress models and equations (7)–(8). For stress model *A* (Figure 5), for instance, the average value of  $\dot{\epsilon}_{xz}$  in the depth range of normal-faulting earthquakes is  $1.3 \times 10^{-17}$  s<sup>-1</sup> in lithosphere younger than 15 m.y. and  $3.2 \times 10^{-18}$  s<sup>-1</sup> for lithosphere 15–35 m.y. old. Within the thrust-faulting field of model *D*,  $\dot{\epsilon}_{xz}$  averages  $2.8 \times 10^{-18}$  s<sup>-1</sup>. These values are comparable to or larger than the average strain rates indicated by the rate of seismic moment release. We conclude that thermal strain is sufficient to account for the seismic strain observed in young oceanic lithosphere in the last two decades.

#### Possible Improvements to Thermal Stress Models

While the comparison of stress predicted by the simple models of this paper to the mechanisms, distribution, and moments of near-ridge earthquakes supports the hypothesis that thermoelastic stress is an important contributor to the earthquake-generating stress field in young oceanic lithosphere it is important to recall the limitations of the modeling scheme adopted here and to suggest alternative approaches that might be pursued in future models. The elastic half-space assumption, for instance, is probably not applicable near the ridge axis. Were the ridge axis modeled as a free surface or as a wedge of ductile material,  $\sigma_{xx}$  in the elastic part of very young lithosphere should be less extensional than in the elastic half-space solution. This is because the ridge axis would not act to restrict strain in the  $x$  direction and thermal contraction on one side of the ridge would not be transmitted to the other side. Whether thrust faulting in the uppermost lithosphere would be predicted in such models without the presence of a cooled surface layer remains to be demonstrated.

The half-space model for thermal stress is also inappropriate near transform faults. If transforms act to localize relief of stress, then  $\sigma_{yy}$  in the uppermost part of the adjoining lithosphere may be less extensional than in the half-space solution. Incorporation of such effects might lead to the prediction of thrust faults with  $P$  axes more nearly perpendicular to the spreading direction, in contrast to the restriction of predicted  $P$  axes in the thrust-faulting domain to the  $x - z$  plane in our two-dimensional models. A transform with significant offset

would also be the site of significant heat conduction in the  $y$  direction. Three-dimensional models of temperature and thermal stress are necessary to assess the significance of this effect.

A major simplification imposed in all of the models presented here is that the characteristic time for release of accumulated thermal stress is a constant, independent of depth and age. It is more likely, however, that stress release is governed by criteria for failure and flow that vary with depth, age, and mode of deformation [e.g., *Goetze and Evans*, 1979; *Brace and Kohlstedt*, 1980]. It would be worthwhile in future models of thermal stress in oceanic lithosphere to consider a stress release scheme based on strength envelopes and internally consistent strain rates and differential stresses.

Also neglected in the simple models of this paper are the potentially important contributions of heterogeneous material properties and thermally induced bending. As may be seen from (2)–(4) and (7), thermal stress is proportional to the product of the coefficient of thermal expansion  $\alpha$  and Young's modulus  $E$  [*Turcotte*, 1974]. Though the variation of these properties in oceanic lithosphere is not well known, available data suggest that  $\alpha E$  in the crust may be as little as half that of the mantle [e.g., *Clark*, 1966]. The lithosphere would then be analogous to a bimetallic strip [*Turcotte*, 1974] in which thermal stress and strain are larger in the uppermost mantle than in the crust. In *Turcotte's* [1974] models, in which  $\sigma_{yy}$  is the only nonzero component of the stress tensor, brittle failure of accumulated stress can induce a bending moment in the plate which places the upper part of the lithosphere under horizontal compression. Thus dissimilar crustal and upper mantle properties may provide an alternative to a hydrothermally cooled surface layer as an explanation of shallow thrust faulting. These alternatives deserve further testing in subsequent models of the thermal stress field in young oceanic lithosphere.

#### CONCLUSIONS

We have presented a set of simple exploratory models to test the hypothesis that thermoelastic stress is a significant component of the stress field in young oceanic lithosphere. The models are based on the response of an elastic half-space to cooling, including in some models the effects of a surficial layer cooled rapidly at or very near the ridge axis by penetrative hydrothermal circulation [*Lister*, 1977]. The stress models have been compared with several key characteristics of near-ridge earthquakes [*Bergman and Solomon*, 1984], including a concentration of moment release in lithosphere younger than 15 m.y. in age, a paucity of seismicity in the crust, and a rough stratification of faulting type, with thrust and strike-slip mechanisms generally confined to depths less than 12 km and normal faulting dominating at greater depth.

The thermal stress models in best agreement with the characteristics of near-ridge earthquakes include a hydrothermally cooled layer 5–10 km thick and a characteristic time for release of stress of several million years. The effects of stress release by fracture and flow are modeled through the inclusion of two parameters, an elastic blocking temperature above which material is presumed not to contribute to the thermal stress field, and a characteristic time for stress release, assumed to be constant throughout the lithosphere. The models of this paper support the hypothesis that thermoelastic stress is a significant contributor to the state of stress in young oceanic lithosphere, but details of the models depend in untested ways on the many simplifying assumptions made. Further testing of this hypothesis with models capable of relaxing one or more of these assumptions is warranted.

*Acknowledgments.* We thank Doug Wiens and Kevin Furlong for constructive reviews of an earlier draft. We are also grateful to Jan Nattier-Barbaro for help in manuscript preparation. This research has been supported by the National Aeronautics and Space Administration under contract NAS 5-27339 and by the National Science Foundation under grant EAR-815908.

## REFERENCES

- Anderson, E. M., *The Dynamics of Faulting*, 2nd ed., 206 pp., Oliver and Boyd, Edinburgh, 1951.
- Anderson, R. N., M. G. Langseth, and J. G. Sclater, The mechanisms of heat transfer through the floor of the Indian Ocean, *J. Geophys. Res.*, **82**, 3391–3409, 1977.
- Artyushkov, E. V., Stresses in the lithosphere caused by crustal thickness inhomogeneities, *J. Geophys. Res.*, **78**, 7675–7708, 1973.
- Bergman, E. A., and S. C. Solomon, Source mechanisms of earthquakes near mid-ocean ridges from body waveform inversion: Implications for the early evolution of oceanic lithosphere, *J. Geophys. Res.*, **89**, 11415–11441, 1984.
- Bergman, E. A., J. L. Nabelek, and S. C. Solomon, An extensive region of off-ridge normal-faulting earthquakes in the southern Indian Ocean, *J. Geophys. Res.*, **89**, 2425–2443, 1984.
- Bott, M. H. P., and N. J. Kusznir, The origin of tectonic stress in the lithosphere, *Tectonophysics*, **105**, 1–13, 1984.
- Brace, W. F., and D. L. Kohlstedt, Limits on lithospheric stress imposed by laboratory experiments, *J. Geophys. Res.*, **85**, 6248–6252, 1980.
- Chen, W.-P., and P. Molnar, Focal depths of intracontinental and intraplate earthquakes and their implications for the thermal and mechanical properties of the lithosphere, *J. Geophys. Res.*, **88**, 4183–4214, 1983.
- Clark, S. P., ed., *Handbook of physical constants*, *Mem. Geol. Soc. Am.*, **97**, 587 pp., 1966.
- Collette, B. J., Thermal contraction joints in a spreading seafloor as origin of fracture zones, *Nature*, **251**, 299–300, 1974.
- Dahlen, F. A., Isostasy and the ambient state of stress in the oceanic lithosphere, *J. Geophys. Res.*, **86**, 7801–7807, 1981.
- Davis, E. E., and C. R. B. Lister, Fundamentals of ridge crest topography, *Earth Planet. Sci. Lett.*, **21**, 405–413, 1974.
- Epp, D., and W. Suyenaga, Thermal contraction and alteration of the oceanic crust, *Geology*, **6**, 726–728, 1978.
- Fleitout, L., and C. Froidevaux, Tectonic stresses in the lithosphere, *Tectonics*, **2**, 315–324, 1983.
- Forsyth, D. W., and S. Uyeda, On the relative importance of driving forces in plate motion, *Geophys. J. R. Astron. Soc.*, **43**, 163–200, 1975.
- Fung, Y. C., *Continuum Mechanics*, 2nd ed., 340 pp., Prentice-Hall, Englewood Cliffs, N. J., 1977.
- Gautschi, W., Error function and Fresnel integrals, in *Handbook of Mathematical Functions*, edited by M. Abramowitz and I. A. Stegun, pp. 295–329, National Bureau of Standards, Washington, D. C., 1964.
- Goetze, C., and B. Evans, Stress and temperature in the bending lithosphere as constrained by experimental rock mechanics, *Geophys. J. R. Astron. Soc.*, **59**, 463–478, 1979.
- Goodier, J. N., On the integration of the thermoelastic equations, *Philos. Mag.*, **7**, 1017–1032, 1937.
- Gregory, R. T., and H. P. Taylor, Jr., An oxygen isotope profile in a section of Cretaceous oceanic crust, Samail ophiolite, Oman: Evidence for  $\delta^{18}\text{O}$  buffering of the oceans by deep (> 5 km) seawater-hydrothermal circulation at mid-ocean ridges, *J. Geophys. Res.*, **86**, 2737–2755, 1981.
- Hager, B. H., and R. J. O'Connell, Kinematic models of large-scale flow in the earth's mantle, *J. Geophys. Res.*, **84**, 1031–1048, 1979.
- Hales, A. L., Gravitational sliding and continental drift, *Earth Planet. Sci. Lett.*, **16**, 31–34, 1969.
- Kostrov, B. V., Seismic moment and energy of earthquakes, and seismic flow of rock, *Izv. Acad. Sci. USSR Phys. Solid Earth*, Engl. Transl., **10**, 13–21, 1974.
- Lewis, B. T. R., The East Pacific Rise and the thermal model, *J. Geophys. Res.*, **88**, 3348–3354, 1983.
- Lilwall, R. C., T. J. G. Francis, and I. T. Porter, Ocean-bottom seismograph observations on the Mid-Atlantic Ridge near 45°N—further results, *Geophys. J. R. Astron. Soc.*, **55**, 255–262, 1978.
- Lister, C. R. B., On the thermal balance of a mid-ocean ridge, *Geophys. J. R. Astron. Soc.*, **26**, 515–555, 1972.
- Lister, C. R. B., Qualitative models of spreading center processes, including hydrothermal penetration, *Tectonophysics*, **37**, 203–218, 1977.
- MacMillan, W. D., *The Theory of the Potential*, 469 pp., McGraw-Hill, New York, 1930.
- McKenzie, D. P., Speculations on the consequences and causes of plate motion, *Geophys. J. R. Astron. Soc.*, **18**, 1–32, 1969.
- McKenzie, D. P., Plate tectonics, in *The Nature of the Solid Earth*, edited by E. C. Robertson, pp. 323–360, McGraw-Hill, New York, 1972.
- McNutt, M., and H. W. Menard, Constraints on yield strength in the oceanic lithosphere derived from observations of flexure, *Geophys. J. R. Astron. Soc.*, **71**, 363–394, 1982.
- Mindlin, R. D., and D. H. Cheng, Thermoelastic stress in the semi-infinite solid, *J. Appl. Phys.*, **21**, 931–933, 1950.
- Molnar, P., Average regional strain due to slip on numerous faults of different orientations, *J. Geophys. Res.*, **88**, 6430–6432, 1983.
- Parsons, B., and J. G. Sclater, An analysis of the variation of ocean floor bathymetry and heat flow with age, *J. Geophys. Res.*, **82**, 803–827, 1977.
- Richardson, R. M., S. C. Solomon, and N. H. Sleep, Tectonic stress in the plates, *Rev. Geophys.*, **17**, 981–1019, 1979.
- Richter, F. M., and B. Parsons, On the interaction of two scales of convection in the mantle, *J. Geophys. Res.*, **80**, 2529–2541, 1975.
- Sandwell, D., and G. Schubert, Lithospheric flexure at fracture zones, *J. Geophys. Res.*, **87**, 4657–4667, 1982.
- Sclater, J. G., C. Jaupart, and D. Galson, The heat flow through oceanic and continental crust and the heat loss of the earth, *Rev. Geophys.*, **18**, 269–311, 1980.
- Smith, A. T., and M. N. Toksoz, Stress distribution beneath island arcs, *Geophys. J. R. Astron. Soc.*, **29**, 289–318, 1972.
- Solomon, S. C., N. H. Sleep, and R. M. Richardson, On the forces driving plate tectonics: Inferences from absolute plate velocities and intraplate stress, *Geophys. J. R. Astron. Soc.*, **42**, 769–801, 1975.
- Stein, S., and E. A. Okal, Seismicity and tectonics of the Ninetyeast Ridge area: Evidence for internal deformation of the Indian plate, *J. Geophys. Res.*, **83**, 2233–2245, 1978.
- Sykes, L. R., and M. L. Sbar, Focal mechanism solutions of intraplate earthquakes and stresses in the lithosphere, in *Geodynamics of Iceland and the North Atlantic Sea*, edited by L. Kristjansson, pp. 207–224, D. Reidel, Hingham, Mass., 1974.
- Timoshenko, S. P., and J. N. Goodier, *Theory of Elasticity*, 3rd ed., 567 pp., McGraw-Hill, New York, 1970.
- Toomey, D. R., S. C. Solomon, G. M. Purdy, and M. H. Murray, Microearthquakes beneath the median valley of the Mid-Atlantic Ridge near 23°N: Hypocenters and focal mechanisms, *J. Geophys. Res.*, **90**, 5443–5458, 1985.
- Turcotte, D. L., Are transform faults thermal contraction cracks?, *J. Geophys. Res.*, **79**, 2573–2577, 1974.
- Turcotte, D. L., Thermal stresses in planetary elastic lithospheres, *Proc. Lunar Planet. Sci. Conf. 13th*, Part 1, *J. Geophys. Res.*, **88**, suppl., A585–A587, 1983.
- Turcotte, D. L., and E. R. Oxburgh, Finite amplitude convective cells and continental drift, *J. Fluid Mech.*, **23**, 29–42, 1967.
- Turcotte, D. L., and E. R. Oxburgh, Mid-plate tectonics, *Nature*, **244**, 337–339, 1973.
- Turcotte, D. L., and G. Schubert, Structure of the olivine-spinel phase boundary in the descending lithosphere, *J. Geophys. Res.*, **76**, 7980–7987, 1971.
- Walcott, R. I., Flexure of the lithosphere at Hawaii, *Tectonophysics*, **9**, 435–446, 1970.
- Watts, A. B., and J. R. Cochran, Gravity anomalies and flexure of the lithosphere along the Hawaiian-Emperor seamount chain, *Geophys. J. R. Astron. Soc.*, **38**, 119–141, 1974.
- Weissel, J. K., R. N. Anderson, and C. A. Geller, Deformation of the Indo-Australian plate, *Nature*, **287**, 284–291, 1980.
- Wiens, D. A., and S. Stein, Age dependence of oceanic intraplate seismicity and implications for lithospheric evolution, *J. Geophys. Res.*, **88**, 6455–6468, 1983.
- Wiens, D. A., and S. Stein, Intraplate seismicity and stresses in young oceanic lithosphere, *J. Geophys. Res.*, **89**, 11442–11464, 1984.

E. A. Bergman and S. C. Solomon, Department of Earth, Atmospheric and Planetary Sciences, Massachusetts Institute of Technology, Cambridge, MA 02139.

S. R. Bratt, Science Applications International Corporation, 10210 Campus Point Drive, San Diego, CA 92121.

(Received November 7, 1984;  
revised May 2, 1985;  
accepted May 24, 1985.)